Coherent and incoherent radiation from high-energy electron and the LPM effect in oriented single crystal

V. N. Baier and V. M. Katkov Budker Institute of Nuclear Physics, Novosibirsk, 630090, Russia

July 9, 2018

Abstract

The process of radiation from high-energy electron in oriented single crystal is considered using the method which permits inseparable consideration of both coherent and incoherent mechanisms of photon emission. The total intensity of radiation is calculated. The theory, where the energy loss of projectile has to be taken into account, agrees quite satisfactory with available CERN data. It is shown that the influence of multiple scattering on radiation process is suppressed due to action of crystal field. Recently authors developed a new approach to analysis of pair creation by a photon in oriented crystals [1]. This approach not only permits to consider simultaneously both the coherent and incoherent mechanisms of pair creation by a photon but also gives insight on the Landau-Pomeranchuk-Migdal (LPM) effect (influence of multiple scattering) on the considered mechanism of pair creation. In the approach the polarization tensor of photon was used which includes influence of both external field and multiple scattering of electrons and positrons in a medium [2]. In the present paper the analysis of process of radiation from a high-energy electron in oriented crystal includes influence of both an external field and the multiple scattering of electron. This makes possible indivisible consideration of both coherent and incoherent mechanisms of photon emission as well as analysis of influence of the LPM effect on radiation process.

The properties of radiation are connected directly with details of motion of emitting particle. The momentum transfer from a particle to a crystal we present in a form $\mathbf{q} = \langle \mathbf{q} \rangle + \mathbf{q}_s$, where $\langle \mathbf{q} \rangle$ is the mean value of momentum transfer calculated with averaging over thermal(zero) vibrations of atoms in a crystal. The motion of particle in an averaged potential of crystal, which corresponds to the momentum transfer $\langle \mathbf{q} \rangle$, determines the coherent mechanism of radiation. The term \mathbf{q}_s is attributed to the random collisions of particle which define the incoherent radiation. Such random collisions we will call "scattering" since $\langle \mathbf{q}_s \rangle = 0$. If the radiation formation length is large with respect to distances between atoms forming the axis, the additional averaging over the atom position should be performed.

Under some generic assumptions the general theory of the coherent radiation mechanism was developed in [3]. If the electron angle of incidence ϑ_0 (the angle between electron momentum **p** and the axis (or plane)) is small $\vartheta_0 \ll V_0/m$, where V_0 is the characteristic scale of the potential, the field E of the axis (or plane) can be considered constant over the pair formation length and the constant-field approximation (magnetic bremsstrahlung limit) is valid. In this case the behavior of radiation probability is determined by the parameter

$$\chi = \frac{\varepsilon}{m} \frac{E}{E_0},\tag{1}$$

where ε is the electron energy, m is the electron mass, $E_0 = m^2/e = 1.32 \cdot 10^{16} \text{ V/cm}$ is the critical field, the system $\hbar = c = 1$ is used. The very important feature of coherent radiation mechanism is the strong enhancement of its probability at high energies (from factor ~ 10 for main axes in crystals of heavy elements like tungsten to factor ~ 170 for diamond) comparing with the Bethe-Heitler mechanism which takes place in an amorphous medium. If $\vartheta_0 \gg V_0/m$ the theory passes over to the coherent bremsstrahlung theory (see [4],[5] [6]). Side by side with coherent mechanism the incoherent mechanism of radiation is acting. In oriented crystal this mechanism changes also with respect to an amorphous medium [7]. The details of theory and description of experimental study of radiation which confirms the mentioned enhancement can be found in [6]. The study of radiation in oriented crystals is continuing and new experiments are performed recently [8], [9].

At high energies the multiple scattering of radiating electron (the LPM effect) suppresses radiation probability when $\varepsilon \geq \varepsilon_e$. In an amorphous medium (or in crystal in the case of random orientation) the characteristic electron energy starting from which the LPM effect becomes essential is $\varepsilon_e \sim 2.5$ TeV for heavy elements [10] and this value is inversely proportional to the density. In the vicinity of crystalline axis (just this region gives the crucial contribution to the Bethe-Heitler mechanism) the local density of atoms is much higher than average one and for heavy elements and at low temperature the gain could attain factor $\sim 10^3$. So in this situation the characteristic electron energy can be $\varepsilon_0 \sim 2.5$ GeV and this energy is significantly larger than "threshold" energy ε_t starting from which the probability of coherent radiation exceeds the incoherent one. It should be noted that the main contribution into the multiple scattering gives the small distance from axis where the field of crystalline axis attains the maximal value. For the same reason the LPM effect in oriented crystals originates in the presence of crystal field and nonseparable from it. This means that in problem under consideration we have both the dense matter with strong multiple scattering and high field of crystalline axis.

Below we consider case $\vartheta_0 \ll V_0/m$. Than the distance of an electron from axis $\boldsymbol{\varrho}$ as well as the transverse field of the axis can be considered as constant over the formation length. For an axial orientation of crystal the ratio of the atom density $n(\varrho)$ in the vicinity of an axis to the mean atom density n_a is

$$\frac{n(x)}{n_a} = \xi(x) = \frac{x_0}{\eta_1} e^{-x/\eta_1}, \quad \varepsilon_0 = \frac{\varepsilon_e}{\xi(0)},$$
(2)

where

$$x_0 = \frac{1}{\pi dn_a a_s^2}, \quad \eta_1 = \frac{2u_1^2}{a_s^2}, \quad x = \frac{\varrho^2}{a_s^2}, \tag{3}$$

Here ρ is the distance from axis, u_1 is the amplitude of thermal vibration, d is the mean distance between atoms forming the axis, a_s is the effective screening radius of the axis potential (see Eq.(9.13) in [6])

$$U(x) = V_0 \left[\ln \left(1 + \frac{1}{x + \eta} \right) - \ln \left(1 + \frac{1}{x_0 + \eta} \right) \right].$$

$$\tag{4}$$

The local value of parameter $\chi(x)$ (see Eq.(1)) which determines the radiation probability in the field Eq.(4) is

$$\chi(x) = -\frac{dU(\varrho)}{d\varrho}\frac{\varepsilon}{m^3} = \chi_s \frac{2\sqrt{x}}{(x+\eta)(x+\eta+1)}, \quad \chi_s = \frac{V_0\varepsilon}{m^3 a_s} \equiv \frac{\varepsilon}{\varepsilon_s}.$$
 (5)

The parameters of the axial potential for the ordinarily used crystals are given in Table 9.1 in [6]. The particular calculation below will be done for tungsten crystals studied in [8]. The relevant parameters are given in Table 1. It is useful to compare the characteristic energy ε_0 with "threshold" energy ε_t for which the radiation intensity in the axis field becomes equal to the Bethe-Maximon one. Since the maximal value of parameter $\chi(x)$:

$$\chi_m = \chi(x_m), \quad x_m = \frac{1}{6}(\sqrt{1 + 16\eta(1+\eta)} - 1 - 2\eta), \quad \chi_m = \frac{\varepsilon}{\varepsilon_m} \tag{6}$$

is small for such electron energy ($\varepsilon_t \ll \varepsilon_m$), one can use the decomposition of radiation intensity over powers of χ (see Eq.(4.52) in [6]) and carry out averaging over x. Retaining three terms of decomposition we get

$$I^{F} = \frac{8\alpha m^{2}\chi_{s}^{2}}{3x_{0}} \left(a_{0}(\eta) - a_{1}(\eta)\chi_{s} + a_{2}(\eta)\chi_{s}^{2} + \ldots\right),$$

$$a_{0}(\eta) = (1+2\eta)\ln\frac{1+\eta}{\eta} - 2,$$

$$a_{1}(\eta) = \frac{165\sqrt{3}\pi}{64} \left[\frac{1}{\sqrt{\eta}} - \frac{1}{\sqrt{1+\eta}} - 4\left(\sqrt{1+\eta} - \sqrt{\eta}\right)^{3}\right],$$

$$a_{2}(\eta) = 64 \left[(1+2\eta)\left(\frac{1}{\eta(1+\eta)} + 30\right) - 12(1+5\eta(1+\eta))\ln\frac{1+\eta}{\eta}\right].$$
 (7)

The intensity of incoherent radiation in low energy region $\varepsilon \leq \varepsilon_t \ll \varepsilon_m$ is (see Eq.(21.16) in [6] and Eq.(A.18) in Appendix A)

$$I^{inc} = \frac{\alpha m^2}{4\pi} \frac{\varepsilon}{\varepsilon_e} g_0 \left[1 + 34.4 \left(\overline{\chi^2 \ln \chi} + 2.54 \overline{\chi^2} \right) \right]$$
$$g_0 = 1 + \frac{1}{L_0} \left[\frac{1}{18} - h \left(\frac{u_1^2}{a^2} \right) \right], \quad \overline{f} = \int_0^\infty f(x) e^{-\frac{x}{\eta_1}} \frac{dx}{\eta_1}, \tag{8}$$

where

$$\varepsilon_{e} = \frac{m}{16\pi Z^{2} \alpha^{2} \lambda_{c}^{3} n_{a} L_{0}}, \quad L_{0} = \ln(ma) + \frac{1}{2} - f(Z\alpha),$$

$$h(z) = -\frac{1}{2} \left[1 + (1+z)e^{z} \text{Ei}(-z) \right], \quad a = \frac{111Z^{-1/3}}{m},$$

$$f(\xi) = \text{Re} \left[\psi(1+i\xi) - \psi(1) \right] = \sum_{n=1}^{\infty} \frac{\xi^{2}}{n(n^{2}+\xi^{2})},$$
(9)

here $\psi(z)$ is the logarithmic derivative of the gamma function, $\operatorname{Ei}(z)$ is the integral exponential function, $f(\xi)$ is the Coulomb correction. For $\chi = 0$ this intensity differs from the Bethe-Maximon intensity only by the term $h(u_1^2/a^2)$ which reflects the nongomogeneity of atom distribution in crystal. For $u_1 \ll a$ one has $h(u_1^2/a^2) \simeq$ $-(1+C)/2 + \ln(a/u_1)$, C = 0.577.. and so this term characterizes the new value of upper boundary of impact parameters u_1 contributing to the value $\langle \mathbf{q}_s^2 \rangle$ instead of screening radius a in an amorphous medium. Conserving in Eq.(7) only the main (the first) term of decomposition, which corresponds to the classical radiation intensity, neglecting the corrections in Eq.(8) $(g_0 = 1, \chi = 0)$, using the estimate $V_0 \simeq Z\alpha/d$ and Eqs.(3), (5), we get

$$\varepsilon_t \simeq \frac{3L_0 dm^2}{2\pi a_0(\eta)} = 63 \frac{L_0 d}{a_0(\eta)} \text{MeV},\tag{10}$$

where the distance d is taken in units 10^{-8} cm. Values of ε_t found using this estimate for tungsten, axis < 111 >, $d=2.74 \cdot 10^{-8}$ cm are consistent with points of intersection of coherent and incoherent intensities in Fig.1 (see Table 1). For some usable crystals (axis < 111 >, room temperature) one has from Eq.(10)

$$\varepsilon_t(C_{(d)}) \simeq 0.47 \text{ GeV}, \quad \varepsilon_t(Si) \simeq 2.0 \text{ GeV}, \quad \varepsilon_t(Ge) \simeq 1.7 \text{ GeV},$$
(11)

so this values of ε_t are somewhat larger than in tungsten except the diamond very specific crystal where value of ε_t is close to tungsten one.

For large values of the parameter χ_m ($\varepsilon \gg \varepsilon_m$) the incoherent radiation intensity is suppressed due to the action of the axis field. In this case the local intensity of radiation can by written as (see Eq.(7.129) in [6])

$$I^{inc} = \frac{29\Gamma(1/3)}{3^{1/6}2430} \frac{\varepsilon}{\varepsilon_e} \frac{\alpha m^2}{\chi^{2/3}(x)} \left[g_0 + \frac{1}{L_0} \left(0.727 + \frac{\ln \chi(x)}{3} \right) \right].$$
(12)

Here we take into account that

$$\ln \frac{1}{\gamma \vartheta_1} = \ln(ma) \to \ln(ma) - h\left(\frac{u_1^2}{a^2}\right) - f(Z\alpha) = L_0 - \frac{1}{2}.$$
 (13)

Averaging the function $(\chi(x))^{-2/3}$ and $\ln \chi(x)(\chi(x))^{-2/3}$ over x according with Eq.(8) one can find the effective value of upper boundary of the transverse momentum transfer ($\propto m\chi_m^{1/3}$ instead of m) which contributes to the value $\langle \mathbf{q}_s^2 \rangle$. Using the obtained results we determine the effective logarithm L by means of interpolation procedure

$$L = L_0 g, \quad g = g_0 + \frac{1}{6L_0} \ln\left(1 + 70\chi_m^2\right).$$
(14)

Let us introduce the local characteristic energy (see Eq.(2))

$$\varepsilon_c(x) = \frac{\varepsilon_e(n_a)}{\xi(x)g} = \frac{\varepsilon_0}{g} e^{x/\eta_1},\tag{15}$$

In this notations the contribution of multiple scattering into the local intensity for small values of χ_m and $\varepsilon/\varepsilon_0$ has a form (see Eq.(15) in [11])

$$I^{LPM}(x) = -\frac{\alpha m^2}{4\pi} \frac{\varepsilon}{\varepsilon_c(x)} \left[\frac{4\pi\varepsilon}{15\varepsilon_c(x)} + \frac{64\varepsilon^2}{21\varepsilon_c^2(x)} \left(\ln \frac{\varepsilon}{\varepsilon_c(x)} + 2.04 \right) \right].$$
(16)

Integrating this expression over x with the weight $1/x_0$ we get

$$I^{LPM} = \frac{\alpha m^2}{4\pi} \frac{\varepsilon}{\varepsilon_e} g \left[-\frac{2\pi\varepsilon g}{15\varepsilon_0} + \frac{64}{63} \frac{\varepsilon^2 g^2}{\varepsilon_0^2} \left(\ln \frac{\varepsilon_0}{\varepsilon g} - 1.71 \right) \right].$$
(17)

It should be noted that found Eq.(17) has a good accuracy only for energy much smaller (at least on one order of magnitude) than ε_0 (see discussion after Eq.(15) in [11]).

The spectral probability of radiation under the simultaneous action of multiple scattering and an external constant field was derived in [6] (see Eqs.(7.89) and (7.90)). Multiplying the expression by ω and integrating over ω one obtains the total intensity of radiation I. For further analysis and numerical calculation it is convenient to carry out some transformations

- 1. Changing of variables: $\nu \to a\nu/2$, $\tau \to 2t/a$, $(\nu \tau \to \nu t)$.
- 2. Turn the contour of integration over t at the angle $-\pi/4$.

One finds after substitution $t \to \sqrt{2}t$

$$I(\varepsilon) = \frac{\alpha m^2}{2\pi} \int_0^1 \frac{y dy}{1 - y} \int_0^{x_0} \frac{dx}{x_0} G_r(x, y), \quad G_r(x, y) = \int_0^\infty F_r(x, y, t) dt - r_3 \frac{\pi}{4},$$

$$F_r(x, y, t) = \operatorname{Im} \left\{ e^{\varphi_1(t)} \left[r_2 \nu_0^2 (1 + ib_r) \varphi_2(t) + r_3 \varphi_3(t) \right] \right\}, \quad b_r = \frac{4\chi^2(x)}{u^2 \nu_0^2},$$

$$y = \frac{\omega}{\varepsilon}, \quad u = \frac{y}{1 - y}, \quad \varphi_1(t) = (i - 1)t + b_r(1 + i)(\varphi_2(t) - t),$$

$$\varphi_2(t) = \frac{\sqrt{2}}{\nu_0} \tanh \frac{\nu_0 t}{\sqrt{2}}, \quad \varphi_3(t) = \frac{\sqrt{2}\nu_0}{\sinh(\sqrt{2}\nu_0 t)},$$
(18)

where

$$r_2 = 1 + (1 - y)^2, \quad r_3 = 2(1 - y), \quad \nu_0^2 = \frac{1 - y}{y} \frac{\varepsilon}{\varepsilon_c(x)},$$
 (19)

 ω is the photon energy, the function $\varepsilon_c(x)$ is defined in Eq.(15) and $\chi(x)$ is defined in Eq.(5). The expression for the spectral probability of radiation used in the above derivation can be found from the spectral form of Eq.(16) in [1] $(dW/dy = \omega dW/d\varepsilon)$ using the standard QED substitution rules: $\varepsilon \to -\varepsilon$, $\omega \to -\omega$, $\varepsilon^2 d\varepsilon \to \omega^2 d\omega$ and exchange $\omega_c(x) \to 4\varepsilon_c(x)$.

The inverse radiation length in tungsten crystal (axis < 111 >) $1/L^{cr}(\varepsilon) = I(\varepsilon)/\varepsilon$ Eq.(18), well as coherent contribution $1/L^{F}(\varepsilon) = I^{F}(\varepsilon)/\varepsilon$ Eq.(25) and incoherent contribution $1/L^{inc}(\varepsilon) = I^{inc}(\varepsilon)/\varepsilon$ Eq.(27) are shown in Fig.1 for two temperatures T=100 K and T=293 K as a function of incident electron energy ε . In low energy region ($\varepsilon \leq 0.3$ GeV) the asymptotic expressions Eqs.(7) and (8) are valid. One can see that at temperature T=293 K the intensity $I^{F}(\varepsilon)$ is equal to $I^{inc}(\varepsilon)$ at $\varepsilon \simeq 0.4$ GeV and temperature T=100 K the intensity $I^{F}(\varepsilon)$ is equal to $I^{inc}(\varepsilon)$ at $\varepsilon \simeq 0.7$ GeV. The same estimates follow from comparison of Eqs.(7) and (8), see also Eq.(10). At higher energies the intensity $I^F(\varepsilon)$ dominates while the intensity $I^{inc}(\varepsilon)$ decreases monotonically.

The inverse radiation length given in Fig.1 can be compared with data directly only if the crystal thickness $l \ll L^{cr}(\varepsilon)$ (thin target). Otherwise one has to take into account the energy loss. The corresponding analysis is simplified essentially if $l \leq L^{min} = (\max(I(\varepsilon)/\varepsilon))^{-1}$. The radiation length $L^{cr}(\varepsilon)$ varies slowly on the electron trajectory for such thicknesses. This is because of weak dependence of $L^{cr}(\varepsilon)$ on energy in the region $L^{cr}(\varepsilon) \simeq L^{min}$ and the relatively large value of $L^{cr}(\varepsilon) \gg L^{min}$ in the region where this dependence is essential but variation of energy on the thickness l is small. For W, axis < 111 >, T=293 K one has $L^{min} = 320 \ \mu m$ at energy $\varepsilon = 300 \ {\rm GeV}$, see Fig.1. For this situation dispersion can be neglected (see discussion in Sec.17.5 of [6]) and energy loss equation acquires the form

$$\frac{1}{\varepsilon}\frac{d\varepsilon}{dl} = -L^{cr}(\varepsilon)^{-1} \equiv -\frac{I(\varepsilon)}{\varepsilon}.$$
(20)

In the first approximation the final energy of electron is

$$\varepsilon_1 = \varepsilon_0 \exp\left(-l/L^{cr}(\varepsilon_0)\right),\tag{21}$$

where ε_0 is the initial energy. In the next approximation one has

$$\ln \frac{\varepsilon(l)}{\varepsilon_0} = -L^{cr}(\varepsilon_0) \int_{\varepsilon_1}^{\varepsilon_0} L^{cr}(\varepsilon)^{-1} \frac{d\varepsilon}{\varepsilon}.$$
 (22)

If the dependence of $L^{cr}(\varepsilon)^{-1}$ on ε is enough smooth it's possible to substitute the function $L^{cr}(\varepsilon)^{-1}$ by an average value with the weight $1/\varepsilon$:

$$L^{cr}(\varepsilon)^{-1} \to \frac{\varepsilon_0 L^{cr}(\varepsilon_1)^{-1} + \varepsilon_1 L^{cr}(\varepsilon_0)^{-1}}{\varepsilon_0 + \varepsilon_1} \equiv \frac{1}{\overline{L}}.$$
 (23)

Numerical test confirms this simplified procedure. Using it we find

$$\ln\frac{\varepsilon(l)}{\varepsilon_0} = -\frac{L^{cr}(\varepsilon_0)}{\overline{L}}\ln\frac{\varepsilon_0}{\varepsilon_1} = -\frac{l}{\overline{L}}, \quad \frac{\Delta\varepsilon}{\varepsilon_0} = 1 - \exp\left(-\frac{l}{\overline{L}}\right) \equiv \frac{l}{L^{ef}}.$$
 (24)

Enhancement of radiation length (the ratio of Bethe-Maximon radiation length L^{BM} and L^{ef}) in tungsten, axis < 111 >, T=293 K is shown in Fig.2. The curve 1 is for the target with thickness $l = 200 \ \mu m$, where the energy loss was taken into account according using the simplified procedure Eq.(24). The curve 2 is for a considerably more thinner target, where one can neglect the energy loss. The only available data are from [8]. The measurement of radiation from more thin targets is of evident interest.

In order to single out the influence of the multiple scattering (the LPM effect) on the process under consideration, we should consider both the coherent and incoherent contributions. The probability of coherent radiation is the first term ($\nu_0^2 = 0$) of the decomposition of Eq.(18) over ν_0^2 . The coherent intensity of radiation is (compare with Eq.(17.7) in [6])

$$I^{F}(\varepsilon) = \int_{0}^{x_{0}} I(\chi) \frac{dx}{x_{0}}.$$
(25)

Here $I(\chi)$ is the radiation intensity in constant field (magnetic bremsstrahlung limit, see Eqs. (4.50), (4.51) in [6]). It is convenient to use the following representation for $I(\chi)$

$$I(\chi) = i \frac{\alpha m^2}{2\pi} \int_{\lambda - i\infty}^{\lambda + i\infty} \left(\frac{\chi^2}{3}\right)^s \Gamma(1 - s) \Gamma(3s - 1) (2s - 1)(s^2 - s + 2) \frac{ds}{\cos \pi s},$$

$$\frac{1}{3} < \lambda < 1.$$
 (26)

The intensity of incoherent radiation is the second term $(\propto \nu_0^2)$ of the mentioned decomposition. In Appendix A the new representation of this intensity is derived, which is suitable for both analytical and numerical calculation:

$$I^{inc}(\varepsilon) = \frac{\alpha m^2}{60\pi} \frac{\varepsilon}{\varepsilon_0} g \int_0^{x_0} e^{-x/\eta_1} J(\chi) \frac{dx}{x_0},$$
(27)

where $J(\chi)$ is defined in Eq.(A.16).

The contribution of the LPM effect in the total intensity of radiation I Eq.(18) is defined as

$$I^{LPM} = I - I^F - I^{inc} \tag{28}$$

The relative contribution (negative since the LPM effect suppresses the radiation process) $\Delta = -I^{LPM}/I$ is shown in Fig.3. This contribution has the maximum $\Delta \simeq 0.8\%$ at $\varepsilon \simeq 0.7$ GeV for T=293 K and $\Delta \simeq 0.9\%$ at $\varepsilon \simeq 0.3$ GeV for T=100 K or, in general, at $\varepsilon \sim \varepsilon_t$. The left part of the curves is described quite satisfactory by Eq.(17). For explanation of right part of the curves let us remind that at $\varepsilon \gg \varepsilon_m$ the behavior of the radiation intensity at $x \sim \eta_1$ is defined by the ratio of the contributions to the momentum transfer of multiple scattering and that of the external field on the formation length l_f (see Eq.(21.3) in [6])

$$k = \frac{\langle \mathbf{q}_s^2 \rangle}{\langle \mathbf{q} \rangle^2} = \frac{\dot{\vartheta}_s^2 l_f}{(w l_f)^2} \sim \frac{\varepsilon}{\varepsilon_0} \chi_m^{-4/3} = \frac{\varepsilon}{\varepsilon_0} \left(\frac{\varepsilon_m}{\varepsilon}\right)^{4/3},$$
$$\frac{1}{L^F} \sim \frac{\alpha}{l_f} \sim \frac{\alpha m^2}{\varepsilon} \chi_m^{2/3} = \frac{\alpha m^2}{\varepsilon_m} \chi_m^{-1/3},$$
(29)

where w is an acceleration in an external field. The linear over k term determines the contribution into intensity of incoherent process: $1/L^{inc}(\varepsilon \gg \varepsilon_m) \sim k/L^F(\varepsilon) \sim$ $\alpha m^2/(\varepsilon_0 \chi_m^{2/3})$. The LPM effect is defined by the next term of decomposition over $k \ (\propto k^2)$ and decreases with energy even faster than $1/L^{inc}(\varepsilon)$. Moreover one has to take into account that at $\varepsilon \geq \varepsilon_s$ the contribution of relevant region $x \sim \eta_1$ into the total radiation intensity is small and $1/L^F(\varepsilon)$ decreases with the energy growth as $\chi_m^{-1/3}$. For such energies the main contribution gives the region $x \sim \chi_s^{2/3} = (\varepsilon/\varepsilon_s)^{2/3}$ and $1/L^{cr}(\varepsilon)$ increases until energy $\varepsilon \sim 10\varepsilon_s$ (see Fig.1). This results in essential reduction of relative contribution of the LPM effect Δ .

It's instructive to compare the LPM effect in oriented crystal for radiation and pair creation processes. The manifestation of the LPM effect is essentially different because of existence of threshold in pair creation process. The threshold energy ω_m is relatively high (in W, axis < 111 >, $\omega_m \sim 8$ GeV for T=100 K and $\omega_m \sim 14$ GeV for T=293 K). Below ω_m influence of field of axis is weak and the relative contribution of the LPM effect attains 5.5 % for T=100 K [1]. There is no threshold in radiation process and I^F becomes larger than I^{inc} at much lower energy ε_t and starting from this energy the influence of field of axis suppresses strongly the LPM effect. So the energy interval in which the LPM effect could appear is much narrower than for pair creation and its relative contribution is less than 1 % in W, axis < 111 >. Since value of ε_t depends weakly on Z (Eq.(10)), $\varepsilon_m \propto Z^{-1}$ (Eqs.(5), (6)) and $\varepsilon_0 \propto Z^{-2}$ (Eq.(9)) the relative contribution of the LPM effect Δ for light elements significantly smaller. Thus, the above analysis shows that influence of multiple scattering on basic electromagnetic processes in oriented crystal (radiation and pair creation) is very limited especially for radiation process.

Acknowledgments

We are grateful to U.Uggerhoj for data. The authors are indebted to the Russian Foundation for Basic Research supported in part this research by Grant 03-02-16154.

A Appendix

New representation of the intensity of the incoherent radiation in external field, asymptotic expansions

In the expression for the intensity of incoherent radiation enters following integral over photon energy ω (see Eq.(21.21) in [6]):

$$J(\chi) = \int_{0}^{1} \left[y^{2}(f_{1}(z) + f_{2}(z)) + 2(1-y)f_{2}(z) \right] dy, \quad z = \left(\frac{y}{\chi(1-y)} \right)^{2/3}, \quad (A.1)$$

where $y = \omega/\varepsilon$, the functions $f_1(z)$ and $f_2(z)$ are defined in the just mentioned equation in [6]:

$$f_1(z) = z^4 \Upsilon(z) - 3z^2 \Upsilon'(z) - z^3,$$

$$f_2(z) = (z^4 + 3z) \Upsilon(z) - 5z^2 \Upsilon'(z) - z^3,$$
(A.2)

here $\Upsilon(z)$ is the Hardy function:

$$\Upsilon(z) = \int_{0}^{\infty} \sin\left(zt + \frac{t^{3}}{3}\right) dt$$
 (A.3)

Introducing the variable $\eta = y/(\chi(1-y))$ we obtain

$$J(\chi) = \int_{0}^{\infty} \left[\frac{\chi^{3} \eta^{2}}{(1+\eta\chi)^{2}} (f_{1}+f_{2}) + \frac{2\chi}{(1+\eta\chi)} f_{2} \right] \frac{d\eta}{(1+\eta\chi)^{2}}$$
$$= \frac{\chi^{3}}{6} \frac{d^{2}}{d\chi^{2}} (J_{1}(\chi) + J_{2}(\chi)) + \frac{d}{d\chi} (\chi^{2} J_{2}(\chi)),$$
(A.4)

where

$$J_{1,2}(\chi) = \int_{0}^{\infty} f_{1,2}(z) \frac{d\eta}{(1+\eta\chi)^2}, \quad z = \eta^{2/3}.$$
 (A.5)

Integrating Eq.(A.5) by parts we find

$$J_{1,2}(\chi) = \frac{f_{1,2}(\infty)}{\chi} - \frac{2}{3} \int_{0}^{\infty} f'_{1,2}(z) \frac{\eta^{2/3} d\eta}{(1+\eta\chi)}.$$
 (A.6)

Since the integral Eq.(A.6) for separate terms of functions $f'_{1,2}(z)$ diverges, one has to transform it to an another form. We represent the functions $f'_{1,2}(z)$ in terms of derivative of the Hardy functions

$$f_1'(z) = z^2 \Upsilon^{(5)}(z) - 3z \Upsilon^{(4)}, \quad f_2'(z) = z^2 \Upsilon^{(5)}(z) - 5z \Upsilon^{(4)} + 3\Upsilon^{(3)}, \tag{A.7}$$

where we used equations

$$z\Upsilon(z) = \Upsilon''(z) + 1, \quad \Upsilon^{(n+3)}(z) = (n+1)\Upsilon^{(n)} + z\Upsilon^{(n+1)}.$$
 (A.8)

Now we will show that

$$\int_{0}^{\infty} \eta^{2/3} f_{1,2}'(z) d\eta = \frac{3}{2} \int_{0}^{\infty} z^{3/2} f_{1,2}'(z) dz = 0.$$
 (A.9)

Using Eq.(A.7) and integration by parts, one can reduce all the integrals in Eq.(A.9) to the form

$$\int_{0}^{\infty} \Upsilon'(z) \frac{dz}{\sqrt{z}} = \operatorname{Re} \int_{0}^{\infty} \frac{dz}{\sqrt{z}} \int_{0}^{\infty} \tau \exp\left(iz\tau + \frac{i\tau^{3}}{3}\right) d\tau$$
$$= \frac{4}{\sqrt{3}} \operatorname{Re} \left(\int_{0}^{\infty} e^{ix^{2}} dx\right)^{2} = 0.$$
(A.10)

The last equation permits one to rewrite Eq.(A.6) as

$$J_{1,2}(\chi) = \frac{f_{1,2}(\infty)}{\chi} + i_{1,2}(\chi), \quad i_{1,2}(\chi) = \chi \int_{0}^{\infty} f_{1,2}'(z) \frac{z^3 dz}{1 + \chi z^{3/2}}.$$
 (A.11)

Entering in Eq.(A.11) expression $(1+u)^{-1}$ we present as contour integral

$$\frac{1}{(1+u)} = \frac{i}{2} \int_{\lambda-i\infty}^{\lambda+i\infty} \frac{u^s}{\sin \pi s} ds, \quad u = \chi z^{3/2}, \quad -1 < \lambda < 0.$$
(A.12)

Using the standard form of the Hardy function one has

$$\Upsilon^{(n)} = \frac{d^n}{dz^n} \operatorname{Im} \int_0^\infty \exp\left(i\left(z\tau + \frac{\tau^3}{3}\right)\right) d\tau = \operatorname{Im} \int_0^\infty (i\tau)^n \exp\left(i\left(z\tau + \frac{\tau^3}{3}\right)\right) d\tau$$
(A.13)

Substituting in the integral in Eq.(A.11) the functions $f'_{1,2}(z)$ in the form Eqs.(A.7), (A.13) and integrating over the variables z and τ we obtain

$$i_{1,2}(\chi) = \frac{i\pi\chi}{12} \int_{\lambda-i\infty}^{\lambda+i\infty} \left(\frac{\chi}{\sqrt{3}}\right)^s \frac{A_{1,2}(s)}{\Gamma\left(1+s/2\right)} \frac{ds}{\sin^2(\pi s/2)},\tag{A.14}$$

where $\Gamma(s)$ is the gamma function,

$$A_{1}(s) = \Gamma\left(\frac{3s}{2} + 6\right) + 3\Gamma\left(\frac{3s}{2} + 5\right),$$

$$A_{2}(s) = \Gamma\left(\frac{3s}{2} + 6\right) + 5\Gamma\left(\frac{3s}{2} + 5\right) + 3\Gamma\left(\frac{3s}{2} + 4\right).$$
 (A.15)

Substituting Eqs.(A.14), (A.15) into Eq.(A.11) and using Eq.(A.4), we get after change of variable $s \to 2s$, displacement of integration contour and reduction of similar terms the final expression for $J(\chi)$

$$J(\chi) = \frac{i\pi}{2} \int_{\lambda-i\infty}^{\lambda+i\infty} \frac{\chi^{2s}}{3^s} \frac{\Gamma(1+3s)}{\Gamma(s)} R(s) \frac{ds}{\sin^2 \pi s}, \quad -\frac{1}{3} < \lambda < 0$$
(A.16)

where

$$R(s) = 15 + 43s + 31s^2 + 28s^3 + 12s^4.$$
(A.17)

In the case $\chi \ll 1$, closing the integration contour on the right, one can calculate the asymptotic series in powers of χ

$$J(\chi) = 15 + 516\chi^2 \left(\ln \frac{\chi}{\sqrt{3}} - C \right) + 1893\chi^2 + \ldots \simeq 15 \left[1 - 34.4\chi^2 \left(\ln \frac{1}{\chi} - 2.542 \right) \right]$$
(A.18)

In the case $\chi \gg 1$ it is convenient to present the integral Eq.(A.16) in the form

$$J(\chi) = \frac{i}{2} \int_{\lambda-i\infty}^{\lambda+i\infty} \frac{\chi^{2s}}{3^s} \Gamma(1-s) \Gamma(1+3s) R(s) \frac{ds}{\sin \pi s}, \quad -\frac{1}{3} < \lambda < 0$$
(A.19)

Closing the integration contour on the left one obtains the series over the inverse powers of χ

$$J(\chi) = \frac{58\pi\Gamma(1/3)}{81 \cdot 3^{1/6}\chi^{2/3}} + \frac{628\pi 3^{1/6}\Gamma(2/3)}{243\chi^{4/3}} - \frac{13}{\chi^2} \left(\ln\chi - \frac{1}{2}\ln3 - C + \frac{57}{52}\right) + \frac{188\pi\Gamma(1/3)}{81 \cdot 3^{1/6}\chi^{8/3}} + \dots$$
(A.20)

References

- [1] V. N. Baier, and V. M. Katkov, Phys.Lett., A 346 (2005) 359.
- [2] V. N. Baier, and V. M. Katkov, Phys.Lett., A 286 (2001) 299.
- [3] V. N. Baier, V. M. Katkov, and V. M. Strakhovenko, Sov.Phys.JETP 65, 686 (1987).
- [4] G.Diambrini Palazzi, Rev.Mod.Phys.40, 611 (1968).
- [5] M.Ter-Mikaelyan, High-Energy Electromagnetic Processes in Condensed Media (Wiley, NY, 1972).
- [6] V. N. Baier, V. M. Katkov and V. M. Strakhovenko, *Electromagnetic Processes at High Energies in Oriented Single Crystals* (World Scientific Publishing Co, Singapore, 1998).
- [7] V. N. Baier, V. M. Katkov, and V. M. Strakhovenko, phys.stat.solidi(b) 149, 521 (1988).
- [8] K.Kirsenom *et al*, Phys. Rev. Lett., **87**, 054801 (2001).
- [9] A. Baurichter *et al*, Phys. Rev. Lett., **79**, 3415 (1997).
- [10] V. N. Baier, and V. M. Katkov, Phys.Rev., D 62, 036008 (2000).
- [11] V. N. Baier, and V. M. Katkov, Phys.Lett., A 327 (2004) 202.

Figure captions

Fig.1 The inverse radiation length in tungsten, axis < 111 > at different temperatures T vs the electron initial energy. Curves 1 and 4 are the total effect: $L^{cr}(\varepsilon)^{-1} = I(\varepsilon)/\varepsilon$ Eq.(18) for T=293 K and T=100 K correspondingly, the curves 2 and 5 give the coherent contribution $I^{F}(\varepsilon)/\varepsilon$ Eq.(25), the curves 3 and 6 give the incoherent contribution $I^{inc}(\varepsilon)/\varepsilon$ Eq.(27) at corresponding temperatures T.

Fig.2

Enhancement (the ratio L^{BM}/L^{ef}) in tungsten, axis < 111 >, T=293 K. The curve 1 is for the target with thickness $l = 200 \ \mu m$, where the energy loss was taken into account (according with Eq.(24)). The curve 2 is for a considerably more thinner target, where one can neglect the energy loss $(L^{ef} \rightarrow L^{cr})$. The data are from [8].

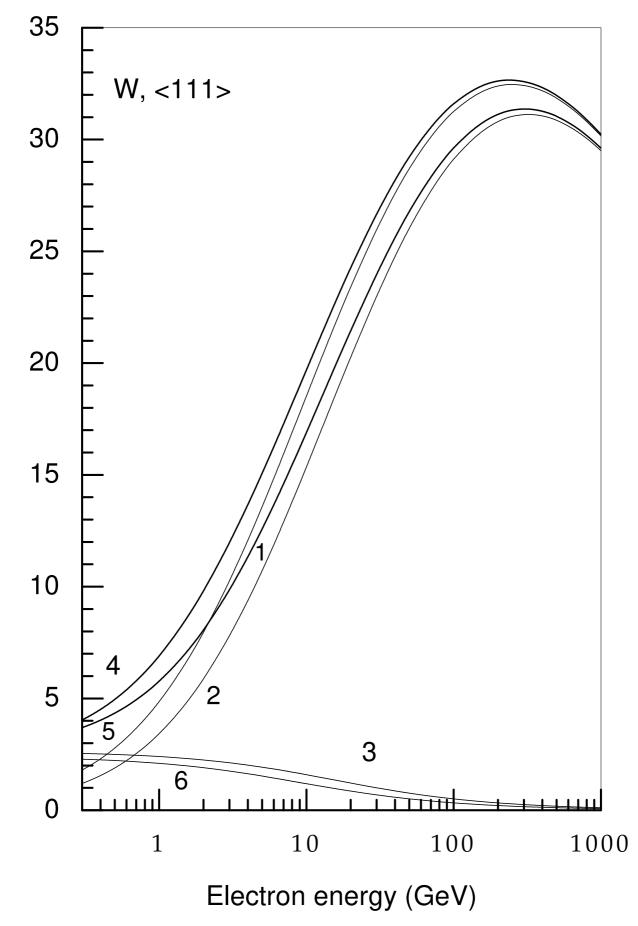
Fig.3

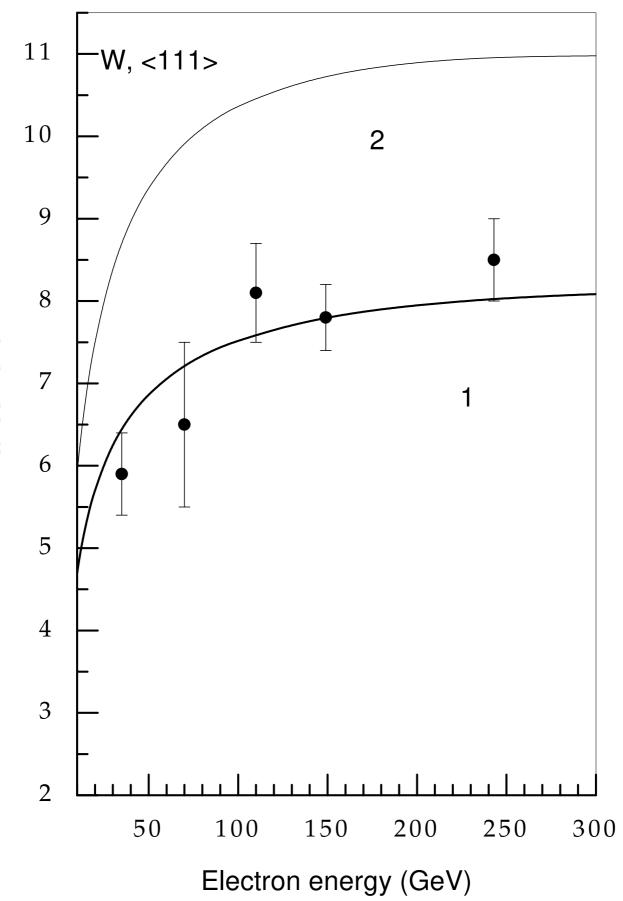
The relative contribution of the LPM effect Δ (per cent) in tungsten, axis < 111 >. Curve 1 is for T=100 K and curve 2 is for T=293 K.

TABLE 1 Parameters of radiation process of the tungsten crystal, axis <111> for two temperatures T

T(K)	$V_0(eV)$	x_0	η_1	η	$\varepsilon_0(\text{GeV})$	$\varepsilon_t(\text{GeV})$	$\varepsilon_s(\text{GeV})$	$\varepsilon_m(\text{GeV})$	h
293	413	39.7	0.108	0.115	7.43	0.76	34.8	14.4	0.348
100	355	35.7	0.0401	0.0313	3.06	0.35	43.1	8.10	0.612

Inverse radiation length (1/cm)





Enhancement



